Hutchinson–Gilford progeria mutant lamin A primarily targets human vascular cells as detected by an anti-Lamin A G608G antibody

Dayle McClintock*, Leslie B. Gordon†, and Karima Djabali*‡

*Department of Dermatology, College of Physicians and Surgeons, Columbia University, New York, NY 10032; and †Department of Pediatrics, Brown Medical School, Providence, RI 02912

Communicated by Francis S. Collins, National Institutes of Health, Bethesda, MD, December 23, 2005 (received for review October 10, 2005)

Hutchinson–Gilford progeria syndrome (HGPS; Online Mendelian Inheritance in Man accession no. 176670) is a rare disorder that is characterized by segmental premature aging and death between 7 and 20 years of age from severe premature atherosclerosis. Mutations in the *LMNA* gene are responsible for this syndrome. Approximately 80% of HGPS cases are caused by a G608 (GGC→GGT) mutation within exon 11 of *LMNA*, which elicits a deletion of 50 aa near the C terminus of prelamin A. In this article, we present evidence that the mutant lamin A (progerin) accumulates in the nucleus in a cellular age-dependent manner. In human HGPS fibroblast cultures, we observed, concomitantly to nuclear progerin accumulation, severe nuclear envelope deformations and invaginations preventable by farnesyltransferase inhibition. Nuclear alterations affect cell-cycle progression and cell migration and elicit premature senescence. Strikingly, skin biopsy sections from a subject with HGPS showed that the truncated lamin A accumulates primarily in the nuclei of vascular cells. This finding suggests that accumulation of progerin is directly involved in vascular disease in progeria.

aging | atherosclerosis

Hutchinson–Gilford progeria syndrome (HGPS) is a rare, fatal genetic disorder that is characterized by accelerated aging in children. The *LMNA* gene encoding the A-type lamins A and C is the causative gene of HGPS (1–3). Approximately 80% of HGPS cases carry the heterozygous silent point mutation G608G within exon 11 of *LMNA* (3). This mutation creates an abnormal splice donor site, which produces a truncated protein (progerin) lacking residues 607–656 of prelamin A but retaining the C-terminal CAAX box, a target for prenylation (1–3).

The nuclear lamina is a scaffold, which provides structural and mechanical stability for the nuclear envelope (NE); it consists primarily of type V intermediate filament proteins (A- and B-type lamins) and many inner-nuclear membrane proteins (4–7). Lamins interact with heterochromatin and transcriptional regulators, suggesting their important role in the maintenance of chromatin organization and gene expression (8).

At the NE periphery, lamin precursors undergo a series of posttranslational modifications. B-type lamins are permanently isoprenylated, whereas prelamin A loses its modification after incorporation into the lamina by lamin A-specific processing steps involving Zmpste24 endoprotease (9–11). Because the endoproteolytic cleavage site is lost in the truncated lamin A (progerin), it was predicted to be permanently prenylated (3). Direct and indirect analyses have recently confirmed that progerin retains the farnesyl group (12–15).

Previous studies of A-type lamin distribution in primary dermal fibroblasts from HGPS patients showed nuclear abnormalities in size and shape in a subpopulation of cells in culture (3, 16, 17). Farnesylated progerin appears to be responsible for the nuclear deformations because administration of farnesyltransferase inhibitors to the HGPS fibroblast cultures normalized the nuclear shape for the majority of the cells *in vitro* (12–15).

The lack of specific tools to directly visualize lamin mutants has so far limited investigating the pathogenesis of laminopathies. The new reading frame of the C-terminal domain of the truncated HGPS lamin A allowed the creation of a specific anti-LMNA G608G Ab. In this article, we report the development of this Ab that recognizes progerin. Immunohistochemistry on biopsied skin sections from an HGPS patient showed that progerin accumulates primarily in the vasculature system; this finding provided a direct link to the disease pathology. Studies on primary dermal fibroblasts from HGPS indicate that progerin accumulates in the nucleus progressively with cellular age. Concomitant to progerin build up in the nuclear lamina, several cellular changes are induced: increased NE invaginations, rapidly decreased growth-rate, premature entry into senescence, and impaired migration potency. These functional changes in HGPS fibroblasts provide preliminary clues about vascular cellular dysfunctions responsible for the progression of atherosclerosis in HGPS subjects.

Results and Discussion

Mutant Lamin A G608G Accumulates Within the Nucleus in a Cellular Age-Dependent Manner as Detected by a Specific Ab. A rabbit polyclonal Ab was raised against a short peptide overlapping the 50-aa deletion region in the mutant lamin A G608G (progerin; see Fig. 6, which is published online as supporting information on the PNAS web site) (17). The immune sera, denoted anti-LMNA G608G, were tested on primary dermal fibroblast cultures at early and late population doublings (PPDs; 20–50) by using four different HGPS fibroblast cultures (see *Materials and Methods*). All four cultures behaved similarly *in vitro*; therefore, results reported herein are derived from HGPS human fibroblasts HGAFN127. Surprisingly, only a few cells were positively labeled with the anti-LMNA G608G Ab at early PPDs (<25; Fig. 1*A*), whereas all nuclei were labeled with anti-emerin Ab that detects an inner-nuclear membrane protein (Fig. 1*A*) (18). Strikingly, the number of nuclei positively stained with anti-LMNA G608G increased with the number of cellular generations *in vitro*. Signal intensity varied; in some cells, it was faint, and in others, it was very bright, indicating that the HGPS fibroblasts contained different amounts of progerin (Fig. 1*A*). Primary dermal fibroblast cultures are asynchronous, suggesting that heterogeneity of anti-LMNA G608G staining reflected cellular age (19). Indeed, Western blot analysis indicated that the progerin product was increased in cultures at late PPDs (Fig. 1*B*),

Conflict of interest statement: No conflicts declared.

Freely available online through the PNAS open access option.

Abbreviations: HGPS, Hutchinson–Gilford progeria syndrome; PPDs, population doublings; NE, nuclear envelope; β-gal, β-galactosidase.

‡To whom correspondence should be addressed. E-mail: kd206@columbia.edu.

www.pnas.org/cgi/doi/10.1073/pnas.0511133103

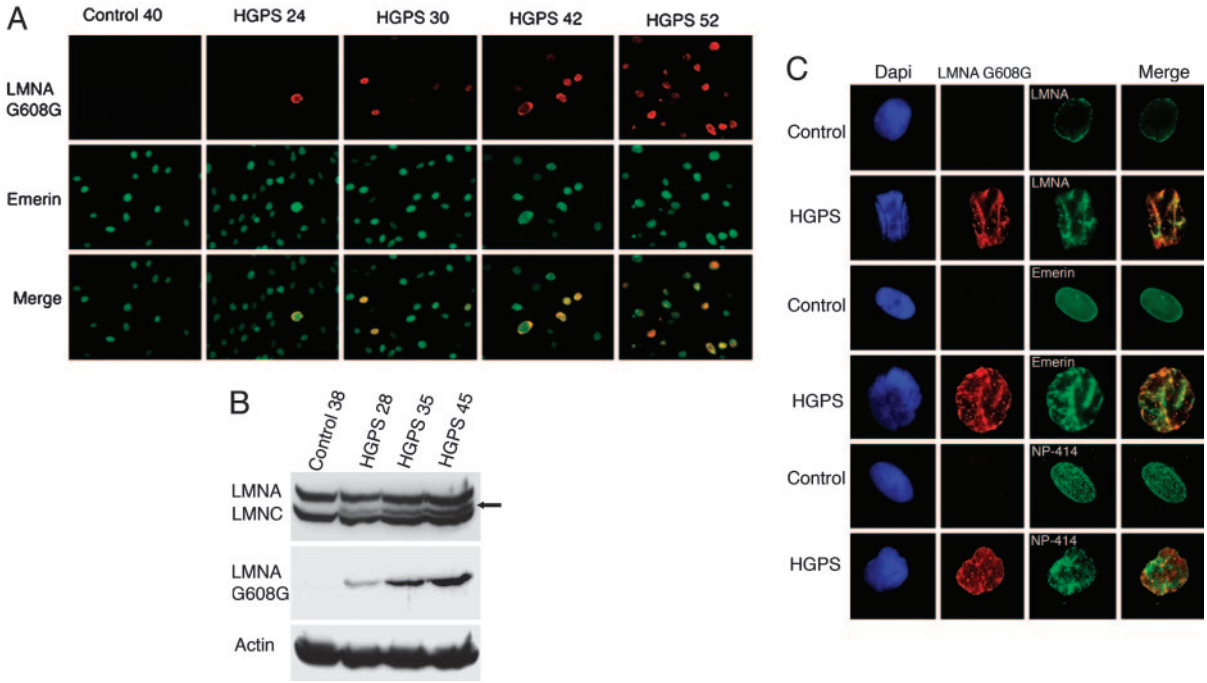

Fig. 1. A unique Ab specifically detects the mutant lamin A G608G (progerin) in HGPS cells and demonstrates the accumulation of the mutant protein progerin over time. (*A*) Immunofluorescence microscopy was performed on fibroblasts from an unaffected individual (40 PPDs) and a subject with HGPS (24, 30, 42, and 52 PPDs). Cells were stained with anti-LMNA G608G (red) and anti-emerin (green); the merged signals are indicated. Note the increase of positively labeled HGPS with increasing PPDs. (*B*) Western blot analysis of control (38 PPDs) and HGPS (28, 35, and 45 PPDs) extracts probed with anti-LMNA G608G and anti-lamin A/C. The arrow indicates the progerin band. (*C*) HGPS and control fibroblasts double-labeled with anti-LMNA G608G (red) and either anti-lamin A, anti-emerin, or anti-nucleoporin 414 (green) reveal the similar distribution into cable-like structures of mutant and wild-type proteins. Chromatin was stained with DAPI (blue).

as reported by using anti-A-type lamin Abs (16). Anti-LMNA G608G serum gave no signal in control dermal fibroblasts by indirect immunofluorescence or by Western blotting (Fig. 1 *A* and *B*).

Progerin Accumulation Induces NE Invaginations. Careful analysis of brightly labeled nuclei with anti-LMNA G608G revealed that the truncated lamin A was distributed in dot-like or cable-like structures (Fig. 1*C*). The intra- and transnuclear cable-like structures detected with anti-LMNA G608G were also labeled with emerin or nucleoporin 414 Abs, suggesting that they associated with the membrane compartment. Furthermore, DAPI staining of mutant nuclei showed severe chromatin rearrangement with the formation of interchromatin folds that coincided with anti-LMNA G608G staining (Fig. 1*C*). These results indicated increased NE invaginations. In nuclei containing low levels of progerin, the mutant protein colocalized with wild-type lamin A and lamin B1 within the nuclear lamina, and emerin and nucleoporin 414 Abs showed a normal distribution pattern (data not shown).

To verify that the cable-like structures were indeed NE invaginations, we performed EM of HGPS cultures at 38 PPDs, where a significant number of cells (25–30%) harbored progerin cable-like distribution as detected by indirect immunofluorescence. EM of ultrathin HGPS sections revealed that 57% of the nuclei showed drastic NE deformations altering the nucleus from a spherical to a lobulated shape; some nuclei remained roughly ovoid but harbored significant intranuclear invaginations (Fig. 2*C*). Those numerous invaginations were composed of a double membrane containing nuclear pores, with some regions exhibiting high pore density; they also remained in close apposition with the nuclear lamina and the chromatin (Fig. 2*D*). In contrast, ultrathin sections of control fibroblast cultures at similar or higher PPDs had ≈22% of the nuclei exhibiting NE invaginations, none as deep or as numerous as in HGPS cells (Fig. 2*A*). Increased NE invaginations have been reported in cells permanently overexpressing prenylated lamins or components of the NE (lamin B receptor or nucleoporin 153), which resembled the ones observed in HGPS fibroblasts at late PPDs (20, 21).

Farnesyltransferase Inhibitor Normalized Nuclear Morphology in HGPS Dermal Fibroblasts. Normal prelamin A processing involves an orchestrated sequence of modifications: farnesylation, carboxyl methylation of the cysteine residue within the CSIM motif, proteolytic cleavage of SIM, and finally cleavage of 15 residues along with its farnesyl moiety to generate the mature lamin A (22). Because last cleavage cannot occur in LMNA G608G, progerin retains its farnesyl group, stabilizing progerin interactions with the inner nuclear membrane (12–15). In this scenario, progerin would force the inward growth of the NE to increase the surface area that can accommodate the excess progerin accumulation in HGPS.

To test the role of farnesylation in HGPS nuclear abnormalities, we treated control and HGPS fibroblast cultures (35–38 PPDs) daily with 20 μM farnesyltransferase inhibitor FTI-277 (23). After a 48-h treatment, the percentage of HGPS nuclei with abnormal shapes decreased from 31% to 8% (Fig. 3*A*). The intranuclear repartition of prelamin A and the localization of LMNA G608G differed greatly between treated and untreated cells; prelamin A was not detectable in untreated control or HGPS cells (Fig. 3*B*). When farnesylation was inhibited in control cells, the lamin A precursor was present in nuclear foci but was mostly accumulated in the lamina where it is assembled, giving rise to a strong nuclear rim staining (Fig. 3*B*), as reported in refs. 23–25. In HGPS fibroblasts treated with FTI-277, the nuclei appeared more ovoid overall, and wild-type prelamin A localization resembled that in control cells (Fig. 3*B*). After a 24-h

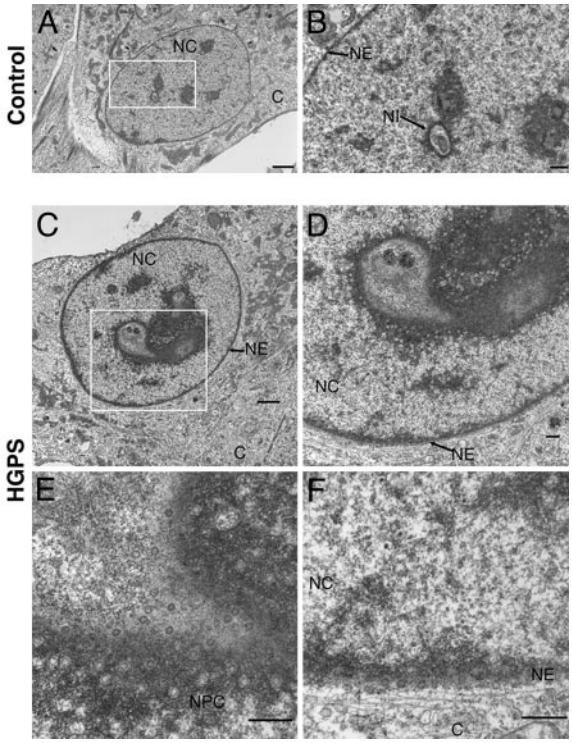

Fig. 2. Progerin accumulation induces NE invaginations as shown by EM on ultrathin sections from control (*A* and *B*) and HGPS (*C–F*) cells at 38 PPDs. Low magnification of control (*A*) and HGPS (*C*) nuclei. (Scale bar, 5 μm.) (*B* and *D–F*) High magnifications of the corresponding nuclei at the NE invaginations (NI). NC, nucleoplasm; C, cytoplasm; NPC, nuclear pore complex. Although few, small nuclear invaginations are detected in control fibroblasts; HGPS nuclei exhibit numerous, large nuclear invaginations recognizable by the presence of a high density of clustered nuclear pores. (Scale bar, 0.5 μm.)

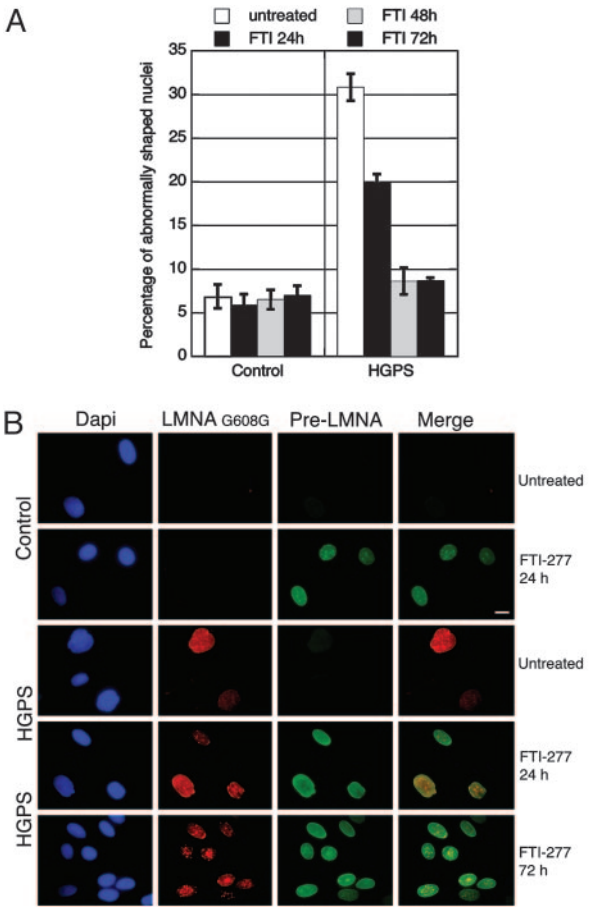

Fig. 3. FTI-277 treatment prevents nuclear deformations and delocalizes progerin. (*A*) Nuclei from control and HGPS cells (35–38 PPDs) were scored for abnormal shape every 24 hours after daily treatment with 20 μM FTI-277 for 3 days and compared against scores for untreated cells. Shown are average percentages of cells with abnormally shaped nuclei for each treatment or time course (error bars at one SD). (*B*) Immunofluorescence microscopy on FTI-277-treated or untreated cells by using anti-LMNA G608G (red), anti-prelamin A (green), and DAPI (blue) demonstrates the gradual relocation of the mutant protein progerin away from the NE and lamina and into intranuclear foci. (Scale bar, 10 μm.)

treatment, anti-LMNA G608G stained the nuclear rim in HGPS fibroblasts, indicating that progerin was still incorporated into the nuclear lamina. Progerin was also detected in nuclear foci similarly to wild-type prelamin A (Fig. 3*B*). After 48 h FTI-277 treatment, however, progerin was progressively depleted from the NE and lamina. Progerin formed large aggregates within the nucleoplasm that sometimes overlapped with the wild-type prelamin A. Seventy-two hours after treatment, whereas wild-type prelamin A was still predominantly detected at the NE and in some nucleoplasmic foci (Fig. 3*B*), progerin was totally depleted from the NE in most nuclei and was localized within nucleoplasmic aggregates (Fig. 3*B*). These results suggest that unfarnesylated progerin lost its ability to bind the NE and to assemble into the lamina, thus restoring a more regular nuclear shape for the majority of the HGPS cells (Fig. 3), as also reported recently in refs. 13, 14, and 26.

Mutant Lamin A Induces Decreased Cellular Proliferation, Premature Senescence, and Altered Motility. During the spatiotemporal expression studies of mutant LMNA G608G, we noticed that the HGPS fibroblasts HGAFN127 grew at the same rate as control cells until they reached ≈40–45 PPDs (Fig. 4*A*). Between 40 and 50 PPDs, as HGPS cells accumulated progerin, their growth rate decreased rapidly until they ceased dividing, between 52 and 57 PPDs under our culture conditions. Late passage control fibroblasts continued to grow and exhibited only a slow decline in their proliferative index when compared with early PPDs (Fig. 4*A*). These observations prompted us to examine whether HGPS cells were entering premature senescence.

Primary cultured cells undergoing cellular senescence *in vitro* express increased β-galactosidase (β-gal) activity when assayed at pH 6 (27). Indeed, when senescence β-gal-positive cells were scored at late PPDs in HGPS cells after 1 week in culture, 3% of the cells were positive, whereas none were detected in control cultures at the same PPDs (Fig. 4*C*). Furthermore, the number of senescent HGPS cells increased with time *in vitro*, reaching 43% after 4 weeks (Fig. 4*C*). In control cells after 4 weeks, one to two senescence β-gal-positive cells could be detected on the entire coverslips. These results indicate that senescent cells accumulated prematurely in HGPS fibroblast cultures. Moreover, when senescence-associated β-gal activity and LMNA G608G levels were assayed on late PPDs of HGPS cells, we observed that senescent cells (β-gal-positive) were brightly labeled with anti-LMNA G608G Ab and harbored nuclear cable-like structures reminiscent of NE invaginations (Fig. 4*D*). This finding indicates that HGPS fibroblasts, concomitantly with the accumulation of mutant lamin A, withdraw from the cell cycle either via the apoptotic pathway as reported in ref. 28 or senescence (Fig. 4*D*).

To gain insight on the cellular effects of progerin, we examined cellular migration, an important function in a variety of physiological aspects. We used a migration assay in which fibroblasts

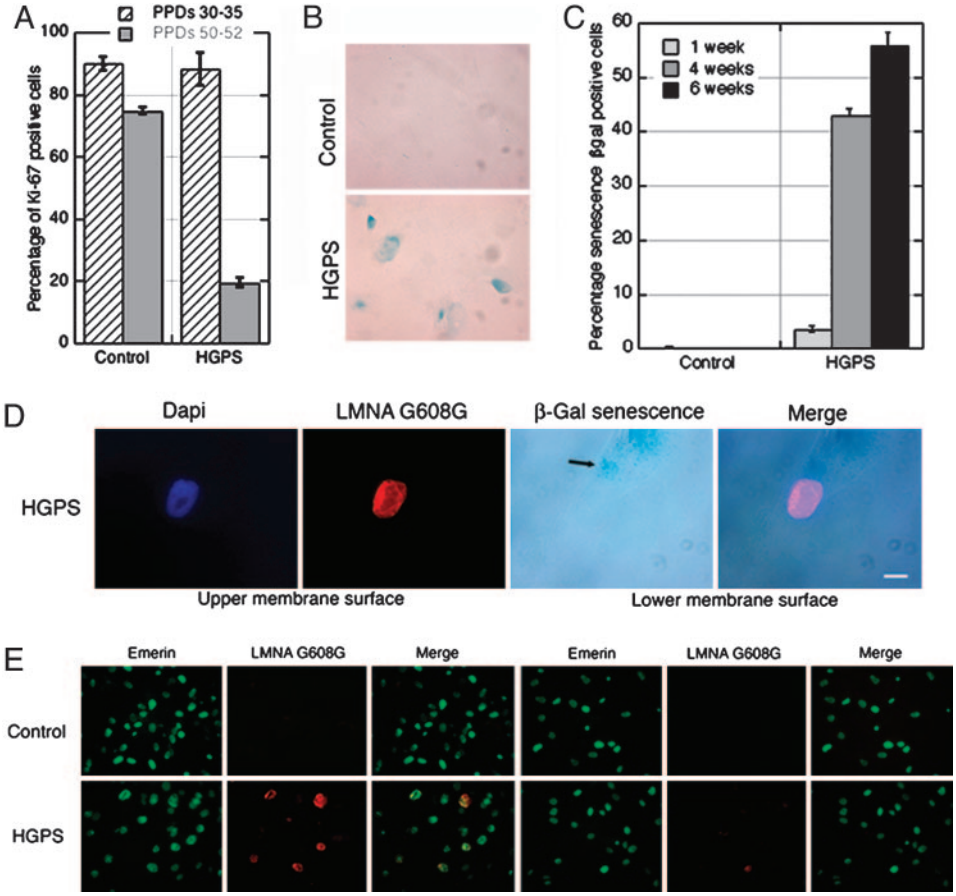

Fig. 4. Mutant LMNA G608G accumulation reduces cellular proliferation, induces premature senescence, and impairs cell migration in HGPS fibroblasts. (*A*) The proliferative index, determined by anti-Ki-67 labeling, was shown to decline faster in HGPS cells than in control cells. (*B*) Senescence β-gal staining revealed more cells of a 4-week-old HGPS culture (55 PPDs) to be senescent versus those of a 1-week-old control culture (55 PPDs). (*C*) The average percentages of cells scored as senescent β-gal-positive from HGPS cells after 1, 4, and 6 weeks (55 PPDs) were significantly higher than 1- and 4-week-old control cultures (55 PPDs). (*D*) HGPS cells (55 PPDs) assayed for senescence-associated β-galactosidase also showed a high level of anti-LMNA G608G signal (red); cells were counterstained with DAPI. (Scale bar, 10 μm.) (*E*) Immunofluorescent labeling of control and HGPS cells (38 PPDs) subjected to migration stimulus revealed an impaired ability to migrate among cells with a bright anti-LMNA G608G signal (red); emerin is green. Merged images are indicated.

could demonstrate both inherent and directional motility in response to a chemotatic stimulus (29). Although the overall number of migrant HGPS cells was similar to controls, none of the migrant HGPS cells were strongly labeled with anti-lamin A G608G Ab (Fig. 4*E*). Indeed, all LMNA G608G brightly positive cells remained on the upper face of the filters where they had been seeded (Fig. 4*E*), associating high progerin levels with reduced migration.

Vascular Cells Are the Primary Targets for Progerin Build-Up, Linking the Mutation to the Pathogenesis of Atherosclerosis in HGPS. Understanding the cellular mechanism underlying the clinical sequelae of HGPS requires the identification of the cellular targets of progerin *in vivo*. Immunohistochemistry was performed on serial frozen sections from a skin biopsy derived from a 9-year-old subject with HGPS (HGADFN143). Hematoxylin/eosin staining showed a well-organized epidermis, a large blood vessel, sweat glands, an arrector pili muscle, and absence of hair follicles (Fig. 5*A*). Connective tissue was very dense with thick fibrous structures throughout the dermis. s.c. fat tissue was absent in this sample. Lamin A/C was detected in the nuclei of most cells from the epidermis and dermis (Fig. 5*A*). The anti-LMNA G608G Ab showed a very restricted pattern of distribution, with positively labeled nuclei localized within the blood vessels, some cells surrounding the sweat glands and in arrector pili muscle. In the epidermis, very few keratinocytes were positively stained with anti-LMNA G608G in the uppermost layer of the epidermis (data not shown). Immunodetection with the LMNA G608G preimmune serum gave no signal, indicating that the signal obtained with anti-LMNA G608G Ab was specific. The anti-LMNA G608G Ab also gave no signal on skin sections from an 86-year-old unaffected individual (Fig. 5*C*). To identify the cell type(s) positively labeled in the blood vessels, we double-labeled HGPS skin sections with anti-LMNA G608G Ab and with anti-α-smooth muscle actin, a reliable marker of smooth muscle cells, or anti-CD31 directed against the endothelial cell surface antigen CD31. We confirmed that the brightest signal obtained with anti-LMNA G608G was indeed located within the vascular system and that the positively labeled nuclei were primarily smooth muscle and endothelial cells (Fig. 5*B*). At high magnification, smooth muscle cell nuclei with a strong LMNA G608G signal adopted similar cable-like structures as HGPS fibroblasts reminiscent of the NE invaginations (data not shown). Thus, we have provided *in vivo* evidence for the presence of progerin in vascular cells. We also have provided support for a direct relation between progerin and atherosclerosis in HGPS.

Previously, autopsies of a few HGPS cases demonstrated severe smooth muscle cell depletion in atherosclerotic aorta media (30, 31). The rare remaining smooth muscle cells had aberrant cellular shape, ballooning mitochondria, and increased

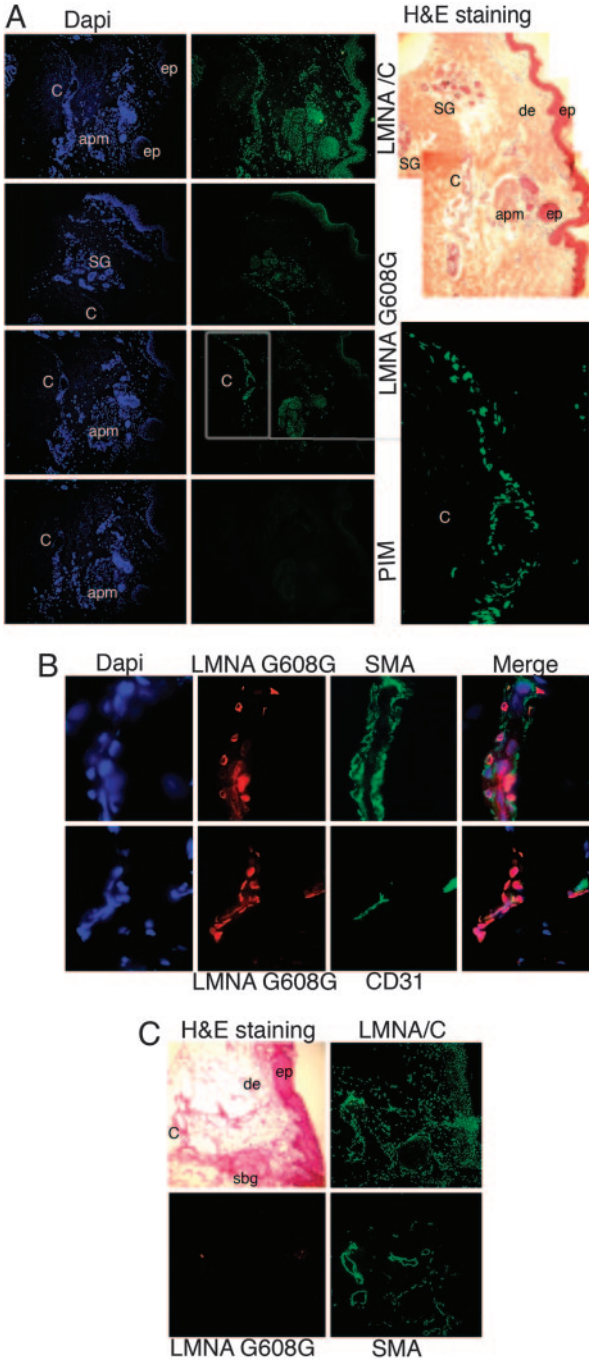

Fig. 5. Mutant lamin A G608G was present mostly in vascular cells on skin sections derived from a subject with HGPS. (*A*) Three serial skin sections were immunostained with anti-lamin A/C Ab, anti-LMNA G608G Ab, or the corresponding preimmune serum. Low magnification, hematoxylin/eosin (H&E) staining: ep, epidermis; de, dermis; SG, sweat glands; C, capillary; apm, arrector pili muscle. Lamin A/C was detected in the nuclei of most cells from the epidermis and in the dermal compartments. Progerin, as detected by anti-LMNA G608G, was restricted to nuclei within the C, some cells surrounding the SG, and the apm. (*Lower Right*) Corresponds to staining with the preimmune serum (PIM) of the rabbit immunized with the LMNA G608G peptide. (*B*) High magnification of blood vessels from HGPS skin sections immunolabeled with anti-LMNA G608G and anti-α-smooth muscle actin (SMA) or anti-CD31 Abs (CD31) and counterstained with DAPI. Triple merged signals are indicated. The mutant lamin A accumulates primarily in the vascular cells, smooth muscle cells, and endothelial cells. (*C*) Normal skin sections immunolabeled with anti-lamin AG608G, anti-lamin A/C, and SMA Abs or stained with hematoxylin/eosin. Note the presence of A-type lamins in most nuclei from the epidermal and dermal compartments. SBG, sebaceous glands.

cytoplasmic density (30). Those observations suggested that smooth muscle cells in HGPS were hypersensitive to hemodynamic and ischemic stress and may become defective in restoring vascular integrity after injury (30). In uninjured blood vessels, smooth muscle and endothelial cells are mostly quiescent. In HGPS subjects, vascular smooth muscle cells may be subjected to increased mechanical stress, forcing them to undergo several cellular divisions to regenerate vascular tissue. The build-up of nuclear progerin may occur as cells reach a high number of PPDs. This phenomenon could be the cause of the detected progerin accumulation in vascular cell nuclei of HGPS skin sections. In such a setting, cells would progressively lose their capacity to grow and migrate and would either become apoptotic or senescent. All those progerin-dependent cellular changes might contribute to the vascular deterioration responsible for the progression of atherosclerosis in HGPS subjects.

In conclusion, this article addresses the *in vivo* cellular and tissue localization of a mutant lamin A (progerin) responsible for severe, premature atherosclerosis in HGPS. Progerin accumulates primarily in vascular cells and can be regarded as a key player in the onset of atherosclerosis, the primary cause of death for HGPS patients. Normalization of cellular function by preventing progerin accumulation, expression, or posttranslational modification by using treatments such as farnesyltransferase inhibitor or genetic therapies (32) show promise as treatments that could significantly reduce disease progression in HGPS children.

Materials and Methods

Characterization of the Anti-Lamin A G608G Ab. The lamin A G608G amino acid sequence reading frame was determined in refs. 1 and 17. To generate a specific anti-Lamin A G608G Ab, we have chosen a short peptide (eight residues; GAQSPQNC) overlapping the region where the 50-residue truncation occurred in the lamin A mutant G608G (see Fig. 6). The peptide was purchased from BioSynthesis (Lewisville, TX); Cocalico Biologicals (Reamstown, PA) immunized two rabbits. Preimmune and immune sera were characterized by Western blot analysis and by indirect immunofluorescence on HGPS and control fibroblasts.

Primary Dermal Fibroblast Cells. We obtained three primary cultures of dermal fibroblasts derived from HGPS patients carrying the *LMNA* mutation G608G: HGADFN001, HGADFN003, and HGAFN127 from the Progeria Research Foundation (Peabody, MA) and PT001 recently identified in ref. 17. We used in parallel three previously established control dermal fibroblast cultures. All results shown in this article correspond to HGPS fibroblasts HGADFN127.

Indirect Immunofluorescence and Western Blot Analysis. Primary cultures of dermal fibroblasts were processed for indirect immunofluorescence as described in ref. 17. Rabbit Abs directed against A-type and B-type lamins were kindly provided by N. Chaudhary (Ridgeway Biosystems, Inc., Cleveland) (33, 34). Goat anti-lamin B1 M-20 and anti-prelamin A C-20 (Santa Cruz Biotechnology), mAbs anti-emerin 4G5 (Novocastra), anti-nucleoporin Nup153 clone 414 (Covance, Richmond, CA), anti-lamin A Jol4 (Serotec, Raleigh, NC), and anti-Ki-67 (BD Bioscience) were purchased. Secondary Abs were affinity purified Alexa Fluor 488 goat or donkey IgG Abs (Molecular Probes) and Cy3-conjugated IgG Abs (Jackson ImmunoResearch). All samples were counterstained with DAPI (Sigma–Aldrich). When cells were treated daily for 3 days with the farnesyltransferase inhibitor FTI-277 (Calbiochem), the culture medium was supplemented with 20 μM FTI-277 or DMSO before immunofluorescence analysis, as described in ref. 23. Images were processed by using ADOBE PHOTOSHOP (Adobe Systems, San Jose, CA). For Western blot analysis, total cellular protein

extracts were isolated from dermal fibroblast cultures at different PPDs (25–55) and processed as described in ref. 17.

***In Vivo* Detection of Lamin A G608G on HGPS Skin Biopsy Sections.** Immunohistochemistry was performed on frozen skin sections from a biopsy of a 9-year-old donor with HGPS carrying the *LMNA* G608G mutation (HGADFN143), provided by the Progeria Research Foundation, and on normal skin sections from an 86-year-old unaffected individual (Columbia University). Frozen sections (6 μm) were fixed by methanol/acetone (1 vol/1 vol) at −20°C for 10 min and processed for indirect immunofluorescence as described above. Rabbit anti-lamin A G608G serum and corresponding preimmune serum were used at a dilution of 1:400, and anti-lamin A/C Ab was used at a dilution of 1:600 (33). Anti- human α-smooth muscle actin, clone 1A4 (DAKO), and anti-CD-31/PECAM-1 Abs (Lab Vision, Fremont, CA) were used according to the manufacturer's instructions. One section was stained with hematoxylin/eosin for morphological comparison.

Cell Migration Assay. Cell migration assays were performed by using standard 8.0-μm pore size transwell inserts (BD Bioscience). Subconfluent HGPS and control dermal fibroblasts from 35–40 PPDs were harvested and resuspended in serum-free DMEM (5×10^5 cells/ml). A cell suspension (500 μl) was added to the upper chamber of the inserts. The lower chamber was filled with 750 μl of DMEM containing 15% FCS. After a 22-h incubation at 37°C, the filters were removed, and the membranes were either processed for upper or lower membrane surfaces for indirect immunofluorescence analysis with anti-lamin A G608G and anti-emerin Abs.

Senescence-Associated β-gal Staining. Dermal fibroblast cultures from 40–45 PPDs were stained for senescence β-gal activity at pH 6 (27). Cells grown on coverslips were fixed in methanol/acetone at −20°C for 5 min, washed in PBS and incubated with anti-lamin A G608G Ab for 1 hour, washed in PBS, and then incubated overnight in fresh senescence β-gal staining solution [1 mg of 5-btomo-4-chloro3-indolyl β-D-galactoside per ml of buffer containing: 40 mM citric acid sodium phosphate, pH 6/0.5 mM potassium ferrocyanide/5 mM potassium ferricyanide/150 mM sodium chloride/2 mM magnesium chloride (27)]. After a 15-h incubation at room temperature, cells were washed in PBS and further processed for indirect immunofluorescence with the secondary Ab.

Quantification. The percentages of Ki-67-positive cells, of misshapen or blebbing nuclei, and senescence β-gal-positive cells were determined by a direct count of 300 cells per coverslip in triplicate and from three independent experiments. The data sets were plotted by using KALEIDAGRAPH (Synergy Software, Reading, PA).

We thank Drs. B. Rost, H. J. Worman, D. Owens, H. Bazzi, A. Morris, C. Jahoda, A. M. Christiano, and D. Bickers for stimulating discussions. The Progeria Research Foundation and National Institutes of Health Grants K01AR048594 and R01AG025302 (to K.D.) supported this work.

1. De Sandre-Giovannoli, A., Bernard, R., Cau, P., Navarro, C., Amiel, J., Boccaccio, I., Lyonnet, S., Stewart, C. L., Munnich, A., Le Merrer, M. & Levy, N. (2003) *Science* **300,** 2055.
2. Cao, H. & Hegele, R. A. (2003) *J. Hum. Genet.* **48,** 271–274.
3. Eriksson, M., Brown, W. T., Gordon, L. B., Glynn, M. W., Singer, J., Scott, L., Erdos, M. R., Robbins, C. M., Moses, T. Y., Berglund, P., *et al.* (2003) *Nature* **423,** 293–298.
4. Fuchs, E. & Weber, K. (1994) *Annu. Rev. Biochem.* **63,** 345–382.
5. Steinert, P. M., Steven, A. C. & Roop, D. R. (1985) *Cell* **42,** 411–420.
6. Aebi, U., Cohn, J., Buhle, L. & Gerace, L. (1986) *Nature* **323,** 560–564.
7. Burke, B. & Stewart, C. L. (2002) *Nat. Rev. Mol. Cell Biol.* **3,** 575–585.
8. Gruenbaum, Y., Goldman, R. D., Meyuhas, R., Mills, E., Margalit, A., Fridkin, A., Dayani, Y., Prokocimer, M. & Enosh, A. (2003) *Int. Rev. Cytol.* **226,** 1–62.
9. Pendas, A. M., Zhou, Z., Cadinanos, J., Freije, J. M., Wang, J., Hultenby, K., Astudillo, A., Wernerson, A., Rodriguez, F., Tryggvason, K. & Lopez-Otin, C. (2002) *Nat. Genet.* **31,** 94–99.
10. Holt, I., Clements, L., Manilal, S., Brown, S. C. & Morris, G. E. (2001) *Eur. J. Hum. Genet.* **9,** 204–208.
11. Krohne, G., Waizenegger, I. & Hoger, T. H. (1989) *J. Cell Biol.* **109,** 2003–2011.
12. Mallampalli, M. P., Huyer, G., Bendale, P., Gelb, M. H. & Michaelis, S. (2005) *Proc. Natl. Acad. Sci. USA* **102,** 14416–14421.
13. Capell, B. C., Erdos, M. R., Madigan, J. P., Fiordalisi, J. J., Varga, R., Conneely, K. N., Gordon, L. B., Der, C. J., Cox, A. D. & Collins, F. S. (2005) *Proc. Natl. Acad. Sci. USA* **102,** 12879–12884.
14. Glynn, M. W. & Glover, T. W. (2005) *Hum. Mol. Genet.* **14,** 2959–2969.
15. Yang, S. H., Bergo, M. O., Toth, J. I., Qiao, X., Hu, Y., Sandoval, S., Meta, M., Bendale, P., Gelb, M. H., Young, S. G. & Fong, L. G. (2005) *Proc. Natl. Acad. Sci. USA* **102,** 10291–10296.
16. Goldman, R. D., Shumaker, D. K., Erdos, M. R., Eriksson, M., Goldman, A. E., Gordon, L. B., Gruenbaum, Y., Khuon, S., Mendez, M., Varga, R. & Collins, F. S. (2004) *Proc. Natl. Acad. Sci. USA* **101,** 8963–8968.
17. Paradisi, M., McClintock, D., Boguslavsky, R. L., Pedicelli, C., Worman, H. J. & Djabali, K. (2005) *Biomed. Cent. Cell Biol.* **6,** 27.
18. Bione, S., Maestrini, E., Rivella, S., Mancini, M., Regis, S., Romeo, G. & Toniolo, D. (1994) *Nat. Genet.* **8,** 323–327.
19. Van Gansen, P. & Van Lerberghe, N. (1988) *Arch. Gerontol. Geriatr.* **7,** 31–74.
20. Prufert, K., Vogel, A. & Krohne, G. (2004) *J. Cell Sci.* **117,** 6105–6116.
21. Ralle, T., Grund, C., Franke, W. W. & Stick, R. (2004) *J. Cell Sci.* **117,** 6095–6104.
22. Weber, K., Plessmann, U. & Traub, P. (1989) *FEBS Lett.* **257,** 411–414.
23. Adjei, A. A., Davis, J. N., Erlichman, C., Svingen, P. A. & Kaufmann, S. H. (2000) *Clin. Cancer Res.* **6,** 2318–2325.
24. Sinensky, M., Beck, L. A., Leonard, S. & Evans, R. (1990) *J. Biol. Chem.* **265,** 19937–19941.
25. Sasseville, A. M. & Raymond, Y. (1995) *J. Cell Sci.* **108,** 273–285.
26. Toth, J. I., Yang, S. H., Qiao, X., Beigneux, A. P., Gelb, M. H., Moulson, C. L., Miner, J. H., Young, S. G. & Fong, L. G. (2005) *Proc. Natl. Acad. Sci. USA* **102,** 12873–12878.
27. Dimri, G. P., Lee, X., Basile, G., Acosta, M., Scott, G., Roskelley, C., Medrano, E. E., Linskens, M., Rubelj, I., Pereira-Smith, O., *et al.* (1995) *Proc. Natl. Acad. Sci. USA* **92,** 9363–9367.
28. Bridger, J. M. & Kill, I. R. (2004) *Exp. Gerontol.* **39,** 717–724.
29. Li, Z., Cheng, H., Ledere, W. J., Froehlich, J. & Lakatta, E. G. (1997) *Exp. Mol. Pathol.* **64,** 1–11.
30. Stehbens, W. E., Wakefield, S. J., Gilbert-Barness, E., Oslon, R. E. & Ackerman, J. (1999) *Cardiovasc. Pathol.* **8,** 29–39.
31. Stehbens, W. E., Delahunt, B., Shozawa, T. & Gilbert-Barness, E. (2001) *Cardiovasc. Pathol.* **10,** 133–136.
32. Scaffidi, P. & Misteli, T. (2005) *Nat. Med.* **11,** 440–445.
33. Chaudhary, N. & Courvalin, J. C. (1993) *J. Cell Biol.* **122,** 295–306.
34. Cance, W. G., Chaudhary, N., Worman, H. J., Blobel, G. & Cordon-Cardo, C. (1992) *J. Exp. Clin. Cancer Res.* **11,** 233–246.